Supporting Information

All-Solid-State Lithium–Sulfur Batteries Enabled by Single-Ion Conducting Binary Nanoparticle Electrolytes

Boram Kim and Moon Jeong Park*
Department of Chemistry, Division of Advanced Materials Science, Pohang University of Science and Technology (POSTECH), Pohang, Korea 37673
E-mail: moonpark@postech.ac.kr

Experimental Section

Materials

Styrene (> 99.9%), divinylbenzene (DVB, 80%), sodium dodecyl sulfate (SDS, > 99.9%), sodium styrene sulfonate (> 90%), (M_w ~1000 kg mol^{-1}, powder), potassium persulfate (KPS, >99.0%), *N,N*-dimethylformamide (DMF, 99.8%), anhydrous acetonitrile (99.8%), 4-dimethylaminopyridine (DMAP, 99.0%), triethylamine (TEA, > 99.0%), sodium bicarbonate (>99.5%), lithium perchlorate (99.99%), poly(ethylene glycol) methyl ether (M_n ~2 kg mol^{-1}), tetrahydrofuran (THF, 99.5%), allyl bromide (99%), sodium hydride (NaH, 95%), 3-mercaptopropyltrimethoxysilane (95%), 4,4'-azobis(4-cyanovaleric acid) (ACVA >98.0%), lithium bis(trifluoromethanesulfonyl)imide (LiTFSI, 98.0%), dimethyl sulfone (DMS, 98%), 1-ethyl-3-methylimidazolium bis(trifluoromethylsulfonyl)imide (EMImTFSI, >97%), sulfur (99.5%), CS_2 (99%), tetrahydroxy-1,4-quinone hydrate (99%), potassium carbonate (K_2CO_3, 99%) were purchased from Sigma-Aldrich. Trifluoromethanesulfonamide (TFSA, >98.0%) and oxalyl chloride (> 98.0%) were purchased from Tokyo Chemical Industry Co., Ltd. Alfa Aesar supplied Super P (> 99%) and *N*-methyl-2-pyrrolidinone (NMP, 99.5%). Ammonia solution (28-30%) was obtained from Samchun.

Synthesis of PS(LiTFSI) NPs

A mixture of styrene (28.8 mmol) and DVB (7.7 mmol) was evenly dispersed in 100 mL of DI water using SDS (1.7 mmol). Subsequently, KPS (0.14 mmol) was added drop by drop. Following 30-min stirring at 70 °C, sodium styrene sulfonate (6.6 mmol) and an additional amount of KPS (0.07 mmol) were added. After 15 min of further stirring, an extra quantity of sodium styrene sulfonate (43.6 mmol) was added dropwise over 1 h. The polymerization proceeded for 16 h at 70 °C, yielding core-crosslinked polystyrene sodium sulfonate nanoparticles (NPs). The $-SO_3^-Na^+$ surface groups of the NPs (2.0 g) were transformed into $-SO_2Cl$ by utilizing oxalyl chloride (1.0 mL) and DMF (0.05 mL) in anhydrous acetonitrile (20 mL). To obtain PS(LiTFSI) shells, PS(SO$_2$Cl) NPs (2 g) were dispersed in acetonitrile, and combined with TFSA (1.5 g), TEA (4 mL), and DMAP (0.5 g) at 0 °C. After 16 h of reaction, a cation exchange reaction with an excess amount of lithium perchlorate in methanol at 60 °C, resulting in the PS(LiTFSI) NPs.

Synthesis of PEO-Grafted Silica NPs (PEO NPs)

Under stirring, a mixture of 3-mercaptopropyltrimethoxysilane (6 mL, 32.3 mmol) and sodium dodecyl sulfate (3.0 g, 10.4 mmol) was dispersed in DI water (150 mL). Once the entire mixture achieved transparency, ammonia solution (15 mL) was added into the reaction flask. The resulting mixtures were then stirred at room temperature overnight. As a result of the described process, silica NPs having thiol surfaces are obtained. The vinyl-terminated PEO was synthesized as follows. Poly(ethylene glycol) methyl ether (2 mmol) was dissolved in anhydrous THF (200 mL) at 50 °C. Allyl bromide (1.2098 g, 10 mmol) and sodium hydride (0.1067, 4 mmol) were then added to the solution. After overnight stirring at 50 °C, the solution was cooled down and subjected to filtration two times to eliminate any remaining unreacted sodium hydride. The thiol-functionalized silica NPs (3.9 g) and vinyl-terminated PEO (3.0 g)

were mixed with ACVA (0.5 g 1.78 mmol) in a flask. Following a 30-min purge with argon gas, thiol-ene click reaction was performed at 75 °C for 24 h. To eliminate any residual PEO, SDS, initiator, and other byproducts, the mixture underwent eight rounds of dialysis against a solution of MeOH/water solution (v/v = 1/2).

Preparation of Binary Polymer Nanoparticles (BNPs) and Control Electrolytes

PS(LiTFSI) NPs and PEO NPs were dispersed in methanol at a concentration of less than 1 wt% and stirred at 70 °C until the solutions became transparent. To prevent NPs aggregation, the NP solutions underwent slow evaporation at 25 °C. The resultant powders were heated, pressed to form freestanding membranes, and then subjected to vacuum-drying. Two types of molds were employed for membrane preparation: a 25 μm thick polyimide film with a 1.9 cm of diameter for Li-S cells and a 250 μm thick silicone spacer with a 1.2 cm of diameter for Li symmetric cells). For the preparation of LiTFSI-doped PEO NPs (1 M LiTFSI in PEO phase), predetermined amounts of LiTFSI and PEO NPs were dissolved in methanol (< 1 wt%) under stirring. The resulting homogenous mixtures were then subjected to vacuum-drying. To prepare PEO/PS(LiTFSI) blends, we employed poly(ethylene glycol) methyl ether (M_n ~2 kg mol^{-1}) that was utilized for the synthesis of PEO NPs. PS(LiTFSI) was synthesized via a two-step modification process of polystyrene sodium sulfonate, which was prepared by aqueous reversible addition-fragmentation chain-transfer polymerization of sodium styrene sulfonate. PEO and PS(LiTFSI) were mixed with varying mass ratios using methanol (< 1 wt%), and subsequently vacuum-dried to obtain the final blends.

Materials Characterizations

The core-shell morphologies and co-assembled structures of PS(LiTFSI) NPs, PEO NPs, and BNPs were assessed using field emission scanning electron microscopy (FE-SEM, XL30S

FEG, Philips) and transmission electron microscopy (TEM, JEM-2200FS, JEOL). To study BNPs superlattices, approximately 300 nm-thick sections of cryo-microtomed BNPs membranes were prepared at -120 °C using RMC Boeckeler PT XL Ultramicrotome. Then, their cross-sectional morphologies were examined using SEM and TEM. The chemical structures and compositions of the NPs were investigated by Fourier transform infrared spectroscopy (FT-IR, Two IR spectrometer, PerkinElmer) and thermogravimetric analysis (TGA, Q50, TA Instruments). Crytallinities of PEO chains in PEO/PS(LiTFSI) blends, PEO NPs, and BNPs electrolytes were determined using differential scanning calorimetry (DSC, Q20, TA Instruments) at heating/cooling rates of 10 °C min^{-1} and X-ray powder diffraction (XRD, Miniflex 600, Rigaku) experiments. Temperature-dependent rheological properties of electrolyte membranes were evaluated using stress-controlled rheometer (DHR-2, TA Instruments) with a parallel plate geometry (0.8 cm of diameter and 0.5 mm of gap size), operating at 0.5 rad s^{-1}, a strain of 0.1%, and heating/cooling rates of 1 °C min^{-1}.

Synthesis of Poly(S-TABQ)

To facilitate the inverse vulcanization reaction, the synthesis of tetra(allyloxy)-1,4-benzoquinone (TABQ) was carried out as follows. A solution of tetrahydoxy-1,4-quinone hydrate (1.10 g) in DMF (20 mL) was prepared, which was added into a solution of K_2CO_3 (3.54 g) in DMF (70 mL). Following 15 min of stirring at 25 °C, a solution of allyl bromide (6.19 g) in DMF was added dropwise into the mixture. The reaction mixtures were heated to 60 °C for 12 h, after which they were cooled down to 0 °C. The products were purified through iterative extraction with CH_2Cl_2, followed by filtration using DI water. To synthesize poly(S-TABQ), elemental sulfur was placed in 20 mL vial and heated to 160 °C under vigorous stirring. As the solid sulfur underwent a phase transition into a molten state, TABQ was slowly

introduced into the molten sulfur. After 3 h, the reaction was quenched by rapidly immersing the vial in liquid nitrogen.

Preparation of Poly(S-TABQ) Cathodes and Li Cells

Slurries were formulated by combining poly(S-TABQ), polyvinylidene difluoride (PVDF, Solvay), and Super P in a mass ratio of 60:30:10 using NMP. As-prepared slurries were coated onto the Al current collect using doctor blading technique. The resulting cathodes were dried under argon blanket at 50 °C for 24 h. The cathode loadings ranged from 1.5 to 2.1 mg cm^{-2}. Coin-type half cells (CR2032, MTI) were fabricated within a glove box filled with high-purity of argon, involving the assembly of lithium foils, electrolytes (25 μm thick), and poly(S-TABQ) cathodes.

Electrochemical Characterizations

Galvanostatic discharge/charge tests and cyclic voltammetry analyses of the fabricated Li cells were conducted using a battery cycler (WBCS3000, Wonatech) within a voltage range of 1.7-2.7 V. Electrochemical impedance spectroscopy (EIS) data were acquired using stainless steel symmetric cells, equipped with a potentiostat (VersaSTAT3, Princeton Applied Research). The electrochemical stability of the was examined by linear sweep voltammetry performed at a scan rate of 1 mV s^{-1} and 40 °C, using a sandwich configuration with lithium foil and stainless steel blocking electrode. Galvanostatic lithium plating/stripping tests were carried out in lithium symmetric cells at 40 °C and 0.1 mA cm^{-2} with a charging/discharging cycle of 1 h. Polarization experiments were conducted at $\Delta V = 0.05$ V and 40 °C, employing lithium/lithium symmetric cells with 250 μm-thick electrolyte membranes.
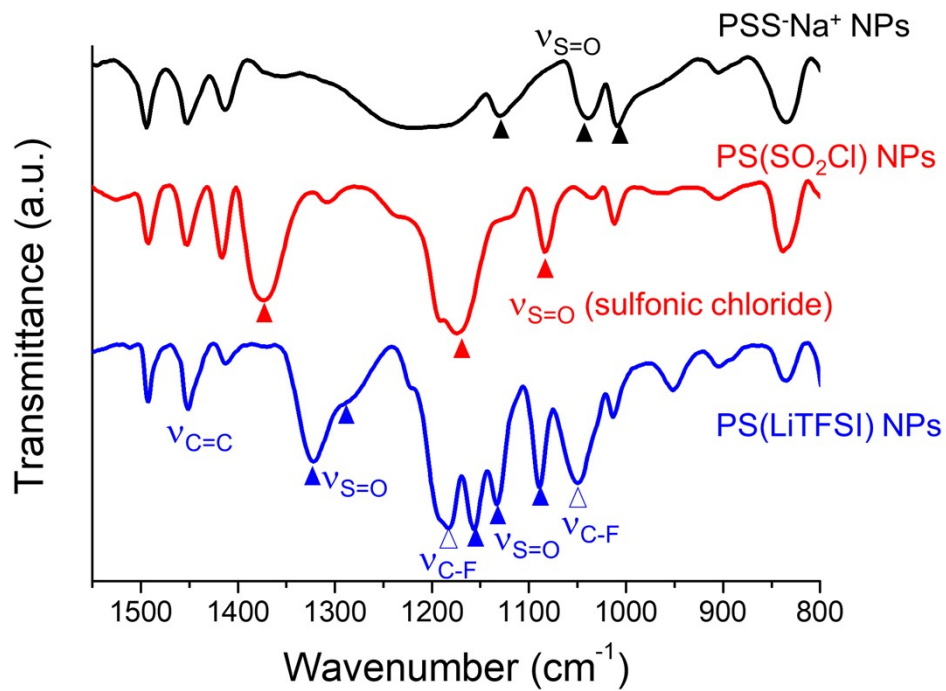
Figure S1. FT-IR spectra of PSS⁻Na⁺ NPs, PS(SO₂Cl) NPs, and PS(LiTFSI) NPs obtained using KBr pellet. The assigned characteristic peaks of the surface functional groups are indicated.
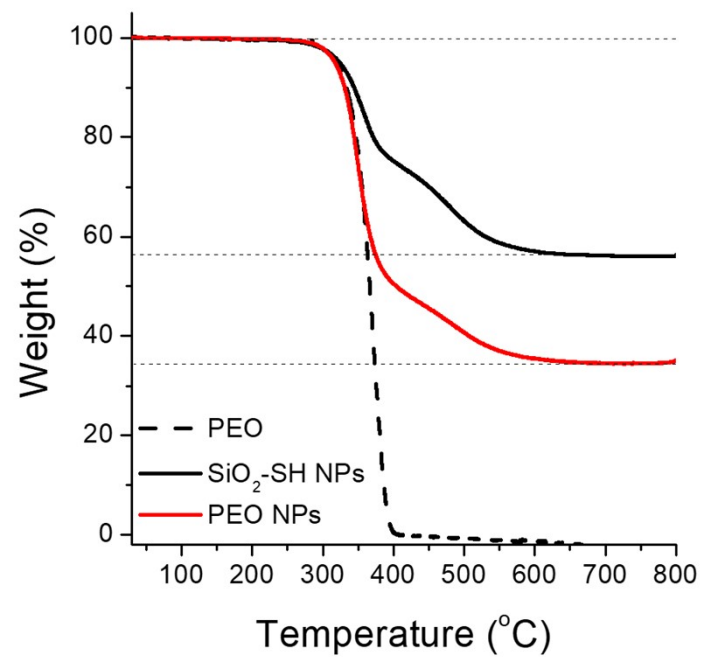
Figure S2. TGA curves of PEO homopolymer, silica nanoparticle with thiol surface (SiO$_2$-SH NP), and PEO-grafted silica nanoparticle (PEO NP).
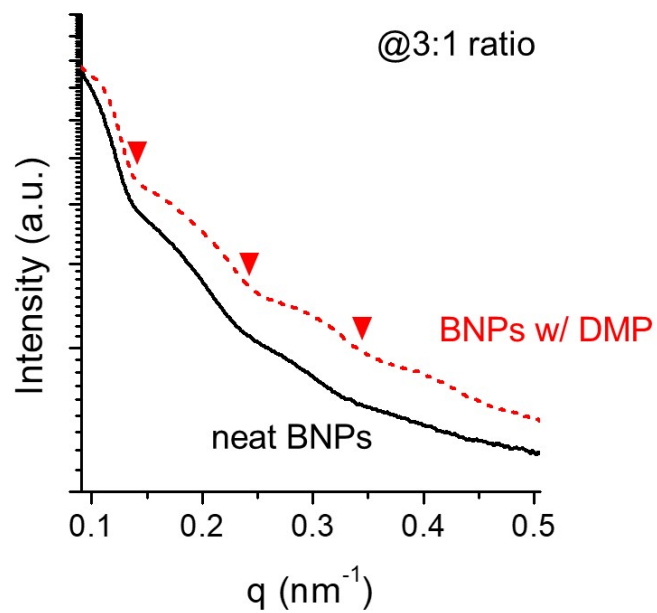
Figure S3. X-ray scattering profiles of neat BNPs (solid line) and BNPs with 4 wt% DMS (dotted red lines), illustrating the minimal influence of DMS on the spacing between PEO NPs within the BNPs. The calculated spacing, indicated by inverted filled triangles, was approximately 64 nm. The first form factor minimum of PS(LiTFSI) NPs at around 0.44 nm^{-1} coincided with the high order fringe of PEO NPs.
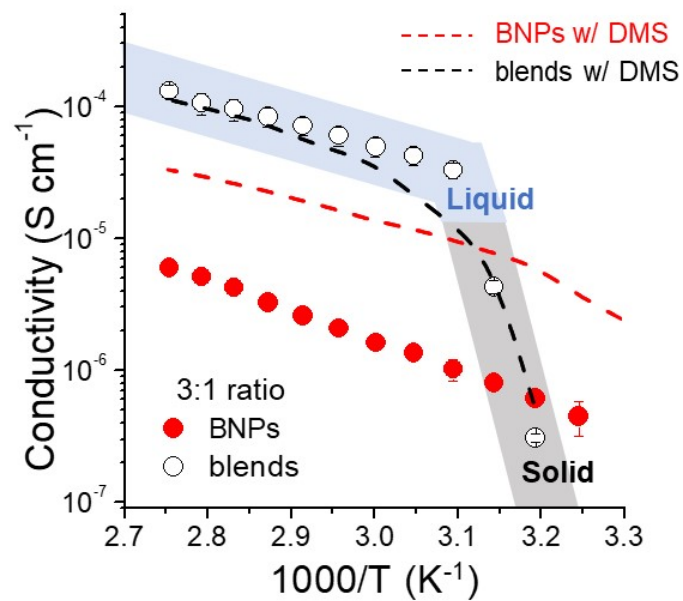
Figure S4. Comparison of ionic conductivities between neat BNPs electrolytes (filled circles) and BNPs electrolytes with 4 wt% DMS (dotted red lines), in relation to PEO/PS(LiTFSI) blend electrolytes without DMS (open symbols) and with 4 wt% DMS (dotted black lines).
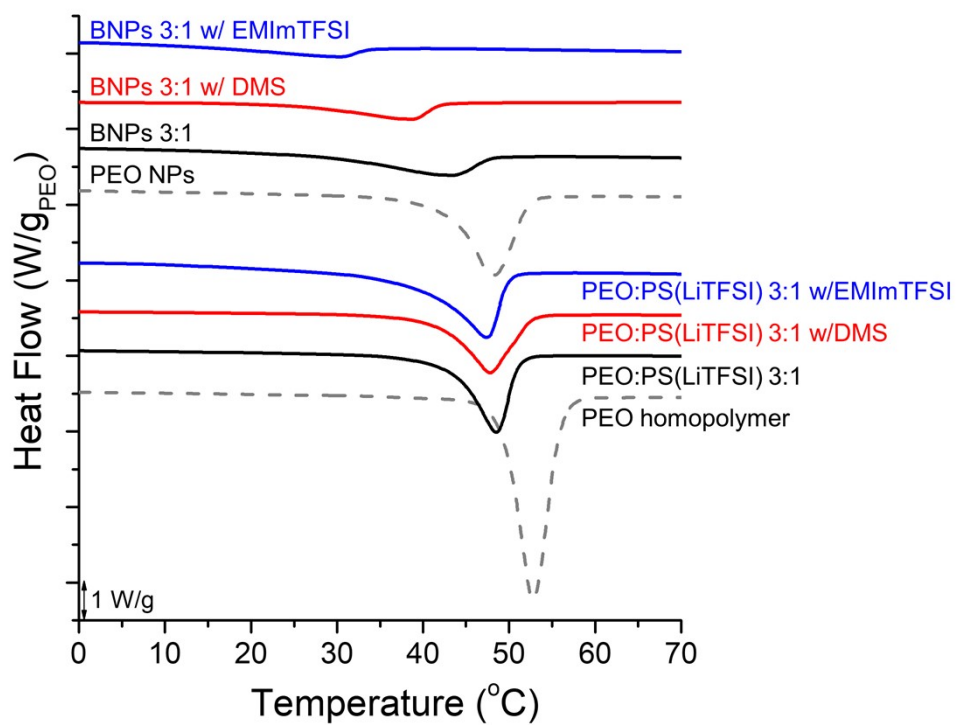
Figure S5. DSC thermograms of neat PEO homopolymer, PEO/PS(LiTFSI) 3:1 blends w/o and w/ additives, neat PEO NPs, and BNPs (PEO NPs/PS(LiTFSI) NPs = 3:1) w/o and w/ additives.
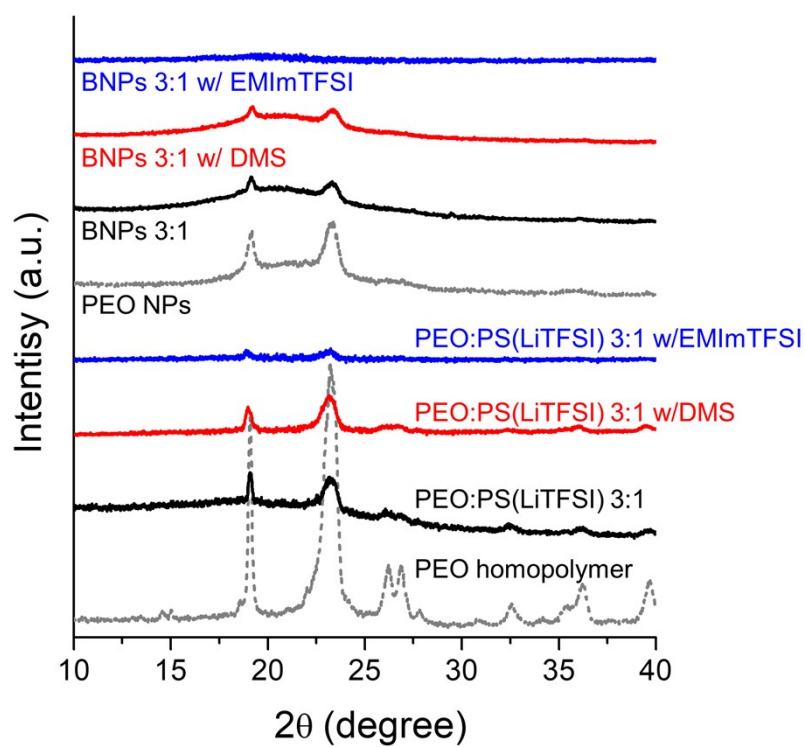
Figure S6. XRD profiles of neat PEO homopolymer, PEO/PS(LiTFSI) 3:1 blends w/o and w/ additives, neat PEO NPs, and BNPs (PEO NPs/PS(LiTFSI) NPs = 3:1) w/o and w/ additives, measured at 25 ℃.
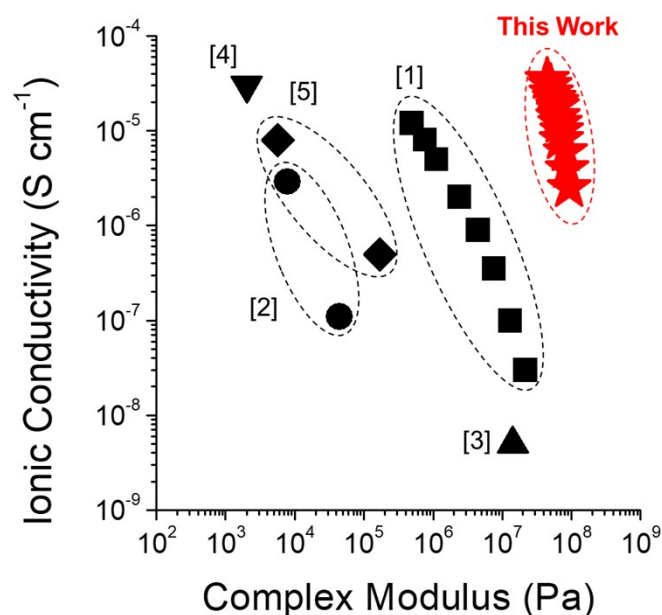
Figure S7. Comparison plot of conductivity–modulus relationship for BNPs electrolytes and solid-state single-ion polymer electrolytes reported in the literature. Quasi-solid electrolytes with lithium salts or liquid additives were excluded from the comparision.

[1] G. Nikolakakou, C. Pantazidis, G.Sakellariou, E.Glynos, *Macromolecules* 2022, **55**, 6131-6139.

[2] G. Lingua, P. Grysan, P. S. Vlasov, P. Verge, A. S. Shaplov, C. Gerbaldi**,** *Macromolecules* 2021, **54**, 6911-6924.

[3] P.-F. Cao, B. Li, G. Yang, S. Zhao, J. Townsend, K. Xing, Z. Qiang, K. D. Vogiatzis, A. P. Sokolov, J. Nanda, T. Saito, *Macromolecules* 2020, **53**, 3591-3601.

[4] L. Meabe, N. Goujon, C. Li, M. Armand, M. Forsyth, D. Mecerreyes, *Batteries & Supercaps* 2020, **3**, 68-75.

[5] E. I. Lozinskaya, D. O. Ponkratov, I. A. Malyshkina, P. Grysan, G. Lingua, C. Gerbaldi, A. S. Shaplov, Y. S. Vygodskii, *Electrochimica Acta* 2022, **413**, 140126.
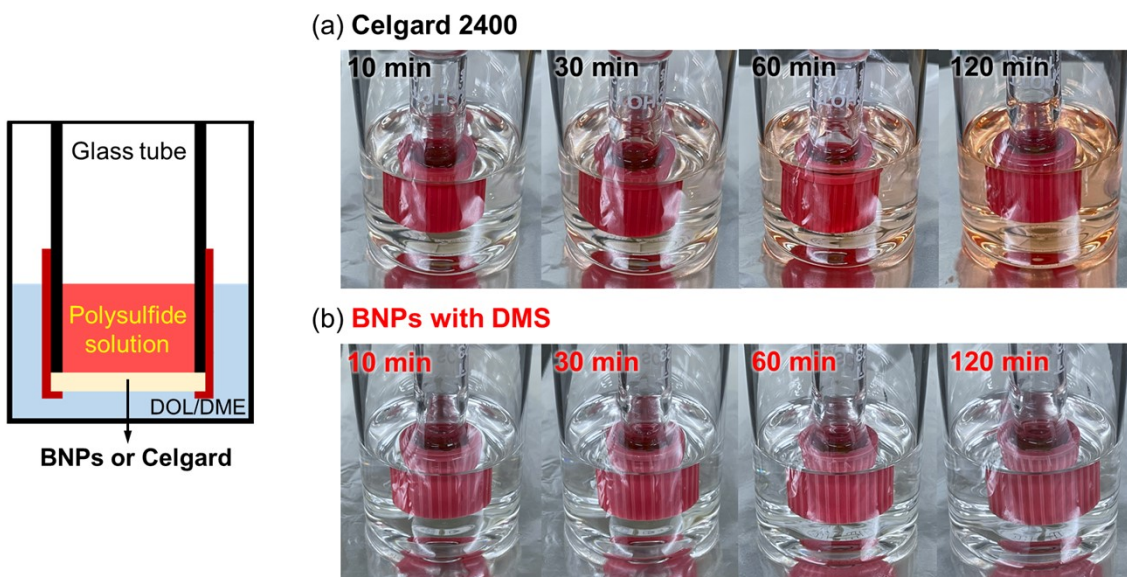
Figure S8. Polysulfide diffusion tests of (a) Celgard 2400 and (b) BNPs electrolytes with different resting times. Photographs show color changes of DOL/DME mixtures containing the commercial propylene separator. This color change occurred within 10 min and gradually intensified over time due to polysulfide elution. In contrast, BNPs electrolytes suppressed the polysulfide shuttle phenomenon, resulting in a stable colorless solution for 120 minutes.
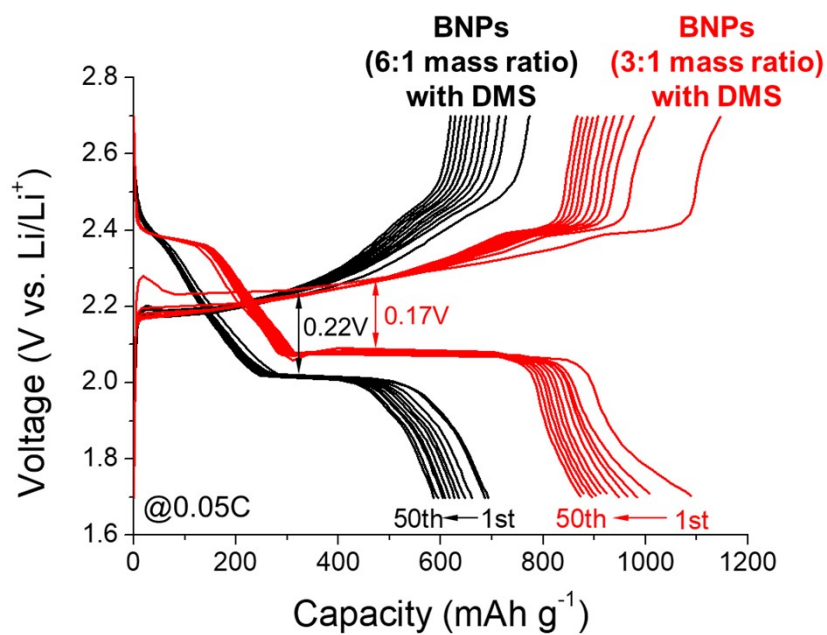
Figure S9. Comparison of galvanostatic charge-discharge voltage profiles for Li/BNPs (3:1 ratio)/S cell at 0.05C and 25 °C, with Li/BNPs (6:1 ratio)/S cell. Both BNPs electrolytes contain 4 wt% of DMS. The results indicate a significant increase in cell polarization from 0.17 to 0.22V, accompanied by a decrease in specific capacity from 1090 to 695 mAh/g during the first cycle.
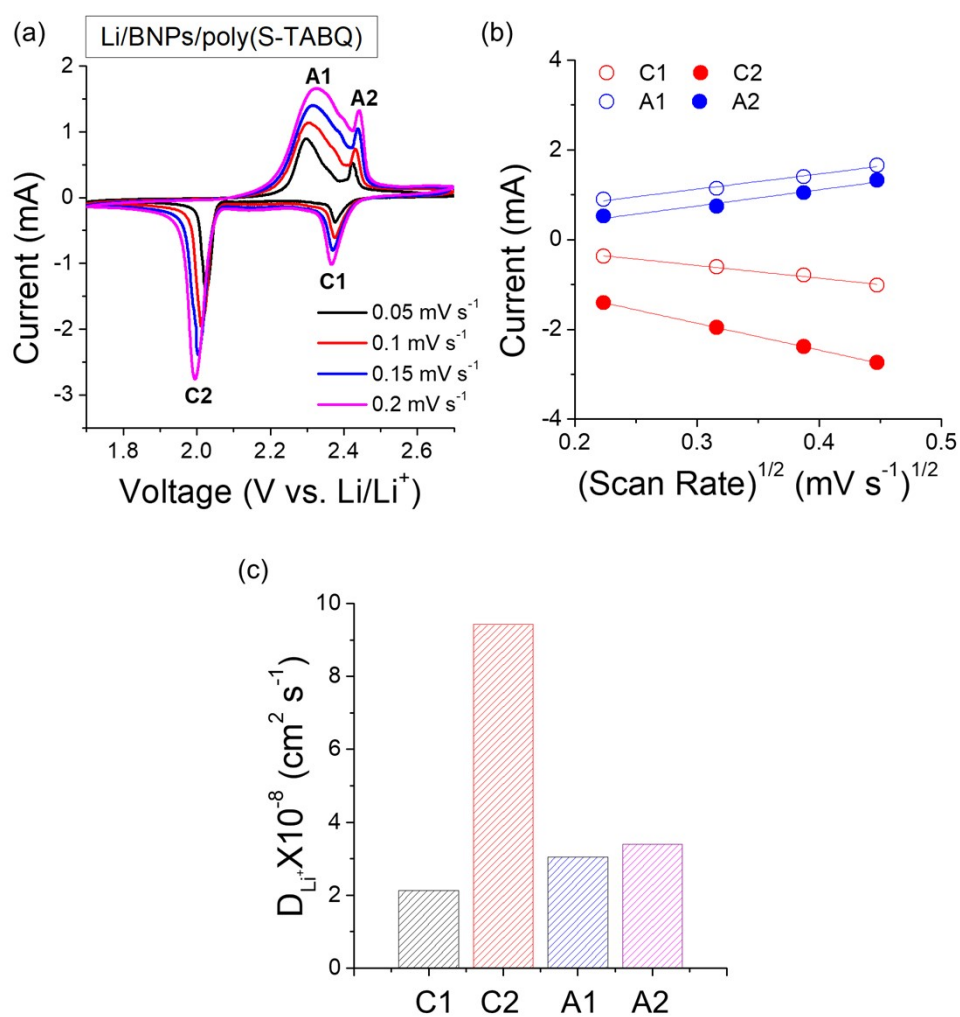
Figure S10. (a) Cyclic voltammograms of Li/BNPs/poly(S-TABQ) cells at different scan rates in the range of 0.05-0.2 mV s^{-1}. (b) Randles-Sevcik analysis results of (a), showing the linear regressions between peak current (I_p) and the square root of the scan rate ($v^{0.5}$). The equation used for the regression is $I_p = 2.69 \times 10^5\ n^{1.5}AD_{Li}^{0.5}v^{0.5}C_{Li}$, where n represents the number of electrons involved in the reaction, A is the electrode area, and C_{Li} is the concentration of Li$^+$ ions in the electrolyte. (c) The calculted diffusion coefficents of Li$^+$ ions (D_{Li}): 2.13×10^{-8} cm^2 s^{-1} and 9.43×10^{-8} cm^2 s^{-1} for cathodic peak currents; 3.05×10^{-8} cm^2 s^{-1} and 3.4×10^{-8} cm^2 s^{-1} for anodic peak currents.
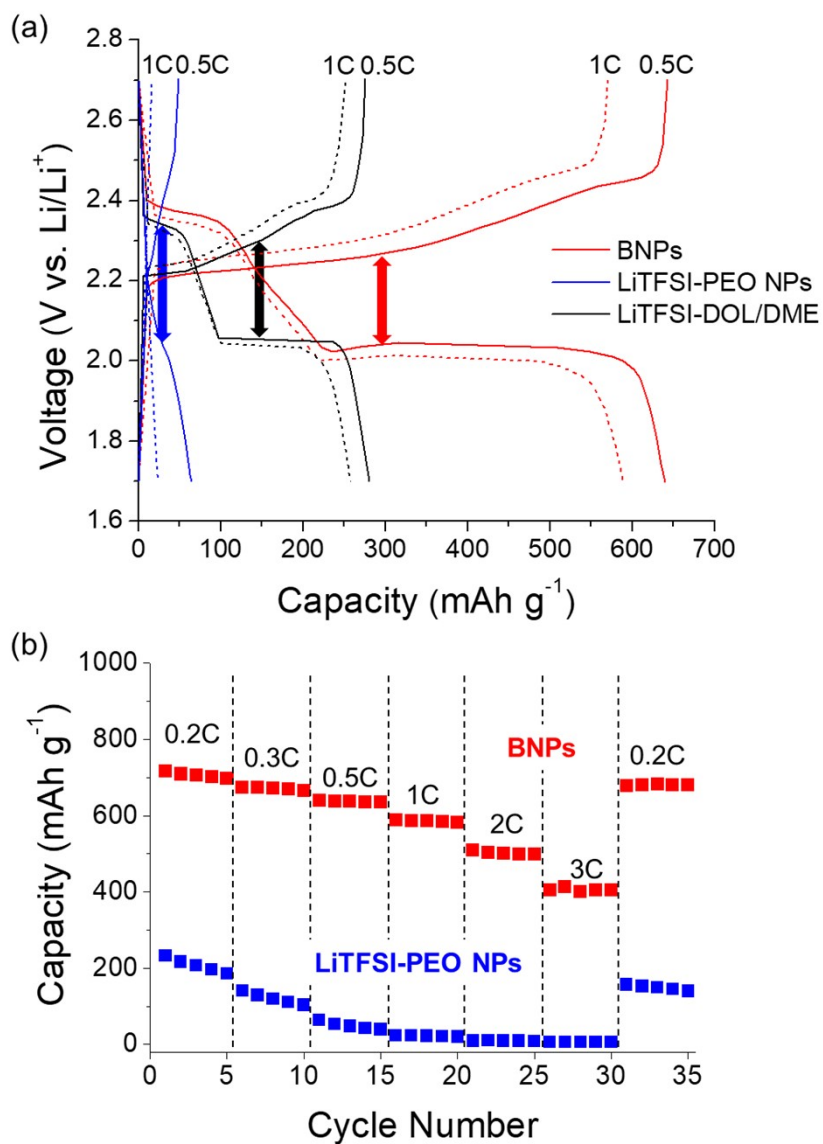
Figure S11. (a) Galvanostatic charge-discharge voltage profiles and (b) rate performance for Li-S cells using BNPs, measured at different C rates and 25 °C. The results obtained with LiTFSI-doped PEO NPs and DOL/DME liquid electrolytes are also shown for comparison.